

# Sensing by Proxy: Occupancy Detection Based on Indoor CO<sub>2</sub> Concentration

Ming Jin, Nikolaos Bekiaris-Liberis, Kevin Weekly, Costas Spanos, Alexandre Bayen

Department of Electrical Engineering and Computer Sciences  
University of California, Berkeley  
Berkeley, California 94720, USA

Emails: {jinning, bekiaris-liberis, kweekly, spanos, bayen}@berkeley.edu

**Abstract**—Sensing by proxy, as described in this study, is a sensing paradigm which infers latent factors by “proxy” measurements based on constitutive models that exploit the spatial and physical features in the system. In this study, we demonstrate the efficiency of sensing by proxy for occupancy detection based on indoor CO<sub>2</sub> concentration. We propose a link model that relates the proxy measurements with unknown human emission rates based on a data-driven model which consists of a coupled Partial Differential Equation (PDE) – Ordinary Differential Equation (ODE) system. We report on several experimental results using both a CO<sub>2</sub> pump that emulates human breathing, as well as measurements of actual occupancy by performing controlled field experiments, in order to validate our model. Parameters of the model are data-driven, which exhibit long-term stability and robustness across all the occupants experiments. The inference of the number of occupants in the room based on CO<sub>2</sub> measurements at the air return and air supply vents by sensing by proxy outperforms a range of machine learning algorithms, and achieves an overall mean squared error of 0.6569 (fractional person), while the best alternative by Bayes net is 1.2061 (fractional person). Building indoor occupancy is essential to facilitate heating, ventilation, and air conditioning (HVAC) control, lighting adjustment, and occupancy-aware services to achieve occupancy comfort and energy efficiency. The significance of this study is the proposal of a paradigm of sensing that results in a parsimonious and accurate occupancy inference model, which holds considerable potential for energy saving and improvement of HVAC operations. The proposed framework can be also applied to other tasks, such as indoor pollutants source identification, while requiring minimal infrastructure expenses.

**Keywords**—Occupancy detection; Building energy efficiency

## I. INTRODUCTION

The thorough understanding of the interaction of occupants and indoor environment has been the key component towards occupancy comforts and energy efficiency of buildings, which account for 40% of total energy usage in the U.S. [1]. Intelligent buildings are conscious about both its occupancy and environment, in order to take controls over its physical systems, such as HVAC and lighting, to optimize user comforts and energy consumption. The knowledge of zone-based occupancy coupled with adaptive building services offers considerable potential for energy reduction [2]–[5].

Many existing methods resort to machine learning algorithms through dense sensor deployment. Various sensors have been employed, including passive infrared (PIR) sensors, read switches, camera [3], [5]–[7], as well as environmental sensors such as acoustics, carbonmonoxide (CO), total volatile organic compounds, small particulates (PM2.5), CO<sub>2</sub>, illumination, temperature, and humidity [6], [8], [9]. Indoor CO<sub>2</sub>

concentration is indicative of the occupancy, as humans are the main source of CO<sub>2</sub> production, although existing approaches suffer from the delay of detection as a result of the relatively long time (10–15minutes) it takes for CO<sub>2</sub> to build up to the corresponding level of concentration [6].

Unlike traditional sensing problems, sensing by proxy has explicit dependency on sensors relative locations as it appears in the computational physics. There are three essential components inherent in the problem, the Location, Link function, and Latent factors, which we call the **L3** factors. In all sensing by proxy systems, the crucial step is to identify these three components and the relationship between them. Location refers to the dependence between sensors location and latent factors. Latent factors, as its name suggests, includes factors that are not directly observable by the sensors and have nonnegligible impact on the system. Link model, a term analogous to the link function from the generalized linear model (GLM) in statistics, refers to the transformation of sensor readings to the quantity of interests. As the design of sensing by proxy systems relies on the identification of the above **L3** factors and their interdependency, the most critical part is the link model, which links location and latent factors and determines the effectiveness of the system.

The key contributions of our work are as follow:

- We develop a link model based on constitutive partial differential equation (PDE) coupled with ordinary differential equation (ODE) that captures the spatial and temporal features of the system and links unobserved human emission to “proxy” measurements of CO<sub>2</sub> concentrations (Section II).
- Our most significant contribution is the design, implementation, and evaluation of occupancy detection algorithm (**Algorithm 1**, Section II) based on the sensing by proxy methodology in controlled and field experiments (Section III). Our method achieves a root mean-squared error (in fractional person) of 0.6311, as compared to 1.2061 by the best alternative strategy (Section IV).

The rest of the paper is organized as follow. The link model is detailed in Section II, which includes the proxy design, modeling, as well as inference. Section III describes the design of CO<sub>2</sub> pump and occupants experiments, whose results are reported in Section IV. Related work is summarized in Section V. Section VI draws conclusion and discusses future works.

## II. SENSING BY PROXY: LINK MODEL

The focus of this section is to introduce the link model in our sensing by proxy framework, which relates the proxy to latent factors and enables the estimation of the latent factors (Section IV).

We start with a description of the PDE-ODE model.

### A. Proxy Design and Modeling

We model the dynamics of the CO<sub>2</sub> concentration in the room using a convection PDE with a source term which models the effect of the CO<sub>2</sub> that is generated by humans. The source term,  $X(t)$ , measured in ppm (part per million), is the output of a linear, time-invariant, scalar, stable ODE system whose input,  $V(t)$ , in ppm/s, represents the unknown humans' emission rate of CO<sub>2</sub> inside the room (within the vicinity of humans), given by

$$\dot{X}(t) = -aX(t) + V(t) \quad (1)$$

where we assume that the unmeasured CO<sub>2</sub> emission rate,  $V(t)$ , from the humans has the form of a piece-wise constant signal,

$$\dot{V}(t) = 0 \quad (2)$$

which is based on our experimental observation that the response of the CO<sub>2</sub> concentration in the room due to changes of the human's CO<sub>2</sub> input has some similarities with the step response of a low-pass filter. The measure of how fast changes to the CO<sub>2</sub> emission rate by the humans affect the CO<sub>2</sub> concentration in the room is specified by the time constant,  $\frac{1}{a}$ , in units of 100s.

The ODE is coupled with a PDE that models the evolution of the CO<sub>2</sub> concentration in the room given by

$$u_t(x, t) = -bu_x(x, t) + b_X X(t) \quad (3)$$

$$u(0, t) = U(t) \quad (4)$$

where  $u(x, t)$  denotes the concentration of CO<sub>2</sub> in the room in ppm at a time  $t \geq 0$  and for  $0 \leq x \leq 1$ , the steady state input CO<sub>2</sub> concentration of the fresh incoming air in ppm is  $U_e$ , and the measured concentration of the fresh incoming air at the air supply vent is the input  $U$  in ppm. Positive parameter,  $b$ , in  $\frac{1}{100s}$ , represents the speed of air convection in the room. The rate of dispersion of CO<sub>2</sub> from the local vicinity of the human to the room is measured by  $b_X$ , in  $\frac{1}{100s}$ , which is a positive number. We scale and center the dimension along the supply-return path so that the air supply is located at  $x = 0$  and the air return is at  $x = 1$ ; therefore, the spatial variable  $x$  is unitless and represents a normalized distance along the path. The CO<sub>2</sub> concentration inside the room at the location of the air supply is represented by  $u(0, t)$ , and the CO<sub>2</sub> concentration inside the room at the location of the air return is given by  $u(1, t)$ .

The evolution of the CO<sub>2</sub> concentration in the room is thus modeled as a linear system, one of whose inputs is the CO<sub>2</sub> concentration of the fresh incoming air measured at the location of the air supply, and the other input is the human emission, if any. The output of the system can be viewed as the CO<sub>2</sub> concentration of the air at the return vent, which is mixed with CO<sub>2</sub> that convects from the air supply towards the air return and the CO<sub>2</sub> that is produced from humans. The concentration of CO<sub>2</sub> at the ceiling in a (non-ratiometric)

normalized distance along an axis from the supply to the return vent is indicated by the value of the PDE on the corresponding interior point of its spatial domain.

The physical representation of our model is illustrated in Figure 1. The convection of air from air supply to the air return vent near the ceiling is represented by the PDE part. The diffusive term is intentionally omitted since it plays a relatively minor role in dispersing indoor pollutants as suggested in [10]. Another design consideration involved is the modeling of the CO<sub>2</sub> concentration near the ceiling since this is where we see most effect from human-generated CO<sub>2</sub>. One explanation is that the warm breath from a human occupant acts as a "bubble" of gas that rises to the ceiling, since it is more buoyant than the ambient, cooler air. Thus, the air coming from lower in the room is modeled as a source term on the PDE across its entire path. The fact that this bubble of air does not immediately rise to the ceiling but only gradually (as observed in the response of the CO<sub>2</sub> concentration in the room due to changes of the human's CO<sub>2</sub> input shown in Figures 5 and 8, during the occupant experiments) is captured by the ODE part of the model, which behaves as a filter between the unknown CO<sub>2</sub> emission rate of humans and the CO<sub>2</sub> concentration in the room.

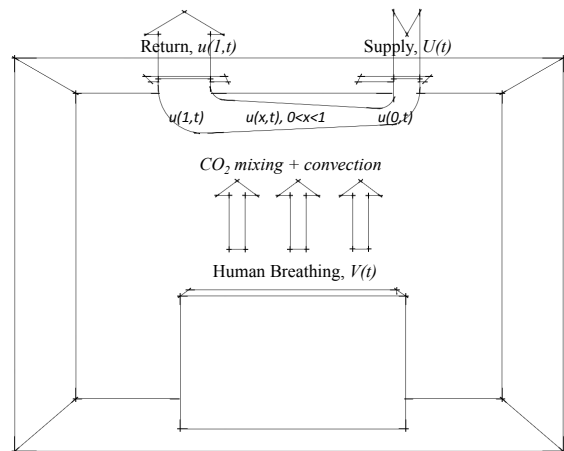


Figure 1. The physical representation of the model. Fresh air with CO<sub>2</sub> concentration  $U(t)$  enters the room from the supply vent, and exits the room after convection and mixing with human breath,  $V(t)$ , which rises to the ceilings, and the measured CO<sub>2</sub> concentration at the return vent is  $u(1, t)$ .

### B. Proxy Inference

The latent factors that are not directly observable are sensed by proxy based on the link model which describes the evolution of proxy under the effects of latent factors. The temporal and spatial dynamics captured by the PDE-ODE link model effectively regularizes the inference output. The approach is clearly different from discriminative models, which assume samples are independent and identically distributed (i.i.d.). It shares some similarities with dynamic Bayesian models such as particle filters (PF) and Conditional Random Field (CRF), which accounts for time evolution of the underlying phenomenon. Nevertheless, proxy inference is directly derived from physical dependency among sensors and is thus more accurate and reliable with provable behaviors as we show next.

The central task in this chapter is to derive an estimation strategy for latent factors, namely the human emission rate  $V(t)$ , based on proxy measurements at the supply vent,  $U(t)$ , and return vent,  $u(1, t)$ . The notation in the derivation follows from the previous description, with a hat to indicate estimation. We consider the following observer, which is a copy of the plant (1)-(4) plus output injection

$$\hat{u}_t(x, t) = -b\hat{u}_x(x, t) + b_X\hat{X}(t) + r(x)(u(1, t) - \hat{u}(1, t)) \quad (5)$$

$$\hat{u}(0, t) = U(t) \quad (6)$$

$$\dot{\hat{X}}(t) = -a\hat{X}(t) + \hat{V}(t) + L_1(u(1, t) - \hat{u}(1, t)) \quad (7)$$

$$\dot{\hat{V}}(t) = -L_2(u(1, t) - \hat{u}(1, t)) \quad (8)$$

The corresponding occupancy detection algorithm is shown in Algorithm 1. The observer design for our PDE-ODE model is based on the design in [11], specifically Theorem 2, which has its origins on the backstepping observer design for some classes of PDEs presented in [12]. We refer the interested reader to [11] for the proof of the following corollary.

*Corollary 1:* Consider the system (1)-(4) and the proxy observer (5)-(8) with

$$r(x) = L_1\pi_1(x) + L_2\pi_2(x) \quad (9)$$

$$\pi_1(x) = \frac{b_X}{a}(e^{\frac{a}{b}x} - 1) \quad (10)$$

$$\pi_2(x) = \frac{b_X}{ba}x + \frac{b_X}{a^2}(1 - e^{\frac{a}{b}x}) \quad (11)$$

Let  $b_X \neq 0$  and choose  $L_1, L_2$  such that the matrix  $A - \begin{pmatrix} L_1 \\ L_2 \end{pmatrix} C$  is Hurwitz, where

$$A = \begin{pmatrix} -a & 1 \\ 0 & 0 \end{pmatrix} \quad (12)$$

$$C = (\pi_1(1) \quad \pi_2(1)) \quad (13)$$

Then for any  $u_0(x), \hat{u}_0(x) \in L_2(0, 1), X(0), \hat{X}(0), V(0), \hat{V}(0) \in \mathbb{R}$ , there exists positive constant  $\lambda$  and  $\kappa$  such that the following holds for all  $t \geq 0$

$$\Omega(t) \leq \kappa\Omega(0)e^{-\lambda t} \quad (14)$$

$$\begin{aligned} \Omega(t) = & \int_0^1 (u(x, t) - \hat{u}(x, t))^2 dx \\ & + (X(t) - \hat{X}(t))^2 + (V(t) - \hat{V}(t))^2 \end{aligned} \quad (15)$$

### III. EXPERIMENTAL DESIGN

#### A. Hardwares

As our approach is not particularly demanding of the accuracy of the proxy measurements, we employ the low-cost K30 CO<sub>2</sub> sensor [13], shown in Figure 2, as the main module in our sensor platform. We implemented a local data storage solution with SD card, and plan to integrate a wireless transmission module in the long run to directly deposit data in our database. The sensor is capable of measuring CO<sub>2</sub> concentrations from 0 to 5000 ppm at a frequency of 1Hz with an accuracy of  $\pm 30$  ppm, or  $\pm 3\%$  of measured value,

---

#### Algorithm 1 Sensing by proxy for Occupancy Detection

---

```

1: function SENSINGBYPROXY( $X^R, X^S, Param$ )
2:   Inputs:  $X^R$ : measurements at air return of size  $1 \times T$ 
3:    $X^S$ : measurements at air supply of size  $1 \times T$ 
4:    $Param$ : hyperparameters
5:   1) Model specification as in Table III: convection
      coefficient  $b$ , source term coefficient  $b_X$ , time
      constant of human effect  $a$ , human emission rate
       $V^H$ , equilibrium concentration in air  $U_e$ 
6:   2) Control parameters:  $L_1, L_2$  as in (7) and (8).
7:   3) Spatial resolution  $d_s$ , temporal resolution  $d_t$ 
8:   4) Smoothing window for median filter:  $w$ 
9:   Initialization:
10:   $\hat{u} \leftarrow U_e \mathbf{1}(d_s, Td_t)$   $\triangleright$  matrix of size  $d_s \times Td_t$ 
11:   $\hat{X} \leftarrow \mathbf{0}(1, Td_t)$   $\triangleright$  vector  $1 \times Td_t$  for emission effect
12:   $\hat{V} \leftarrow \mathbf{0}(1, Td_t)$   $\triangleright$  vector  $1 \times Td_t$  for emission rate
13:   $x^R \leftarrow kron(X^R, \mathbf{1}(1, d_t))$   $\triangleright$  Discretize return/supply
14:   $x^S \leftarrow kron(X^S, \mathbf{1}(1, d_t))$   $\triangleright$  by kronecker product
15:   $\tau \leftarrow \frac{1}{d_t}$   $\triangleright$  time discretization step
16:   $r(n) \leftarrow L_1 \frac{b_X}{a}(e^{a/b} - 1) + L_2(\frac{b_X}{ba} + \frac{b_X}{a^2}(1 - e^{a/b}))$ 
17:  Main program:
18:  for  $t \in \{1, \dots, Td_t\}$  do
19:     $\hat{u}(0, t) \leftarrow x^S(t)$   $\triangleright$  Equ.(6)
20:    for  $n \in \{1, \dots, d_s\}$  do  $\triangleright$  PDE updates
21:       $\hat{u}_x(n, t) \leftarrow (\hat{u}(n, t) - \hat{u}(n-1, t))d_s$   $\triangleright$  spatial
22:       $\hat{u}(n, t+1) \leftarrow \hat{u}(n, t) + \tau \left( -b\hat{u}_x(n, t) + \right.$ 
23:         $\left. b_X\hat{X}(t) + r(n)(x^R(t) - \hat{u}(d_s, t)) \right)$   $\triangleright$  Equ. (5) updates
24:    end for
25:     $\hat{X}(t+1) \leftarrow \hat{X}(t) + \tau \left( -a\hat{X}(t) + \hat{V}(t) + L_1(x^R(t) - \right.$ 
26:       $\left. \hat{u}(d_s, t)) \right)$   $\triangleright$  updates by (7)
27:     $\hat{V}(t+1) \leftarrow \hat{V}(t) + \tau L_2(x^R(t) - \hat{u}(d_s, t))$ 
28:  end for
29:  Outputs:  $y_{Occupants} \leftarrow \lfloor \frac{\text{median}(\hat{V}, w)}{V^H} + \frac{1}{2} \rfloor$   $\triangleright$  round of
30:  signal after median filter with window size  $w$ 
31: end function

```

---

which is considered sufficient for the purpose of occupancy detection.

Sensor calibration is performed by baseline method. We leave the sensors in a well ventilated room with outdoor supply air for few hours. The systematic offset,  $\xi_i$ , is given by

$$\xi_i = \frac{1}{T_{\text{cal}}} \sum_{t=1}^{T_{\text{cal}}} y_t - x_{\text{outdoor}} \quad (16)$$

where  $T_{\text{cal}}$  is the length of the calibration period,  $y_t$  is the sensor reading at time  $t$ , and  $x_{\text{outdoor}}$  is the outdoor CO<sub>2</sub> concentration, usually at 400ppm. The offset  $\xi_i$  is subtracted from sensor  $i$  under the *well mixed assumption*, which states as “at steady state, the air in the room is well mixed, with the CO<sub>2</sub> concentration the same as the fresh air from the air supply vent”.

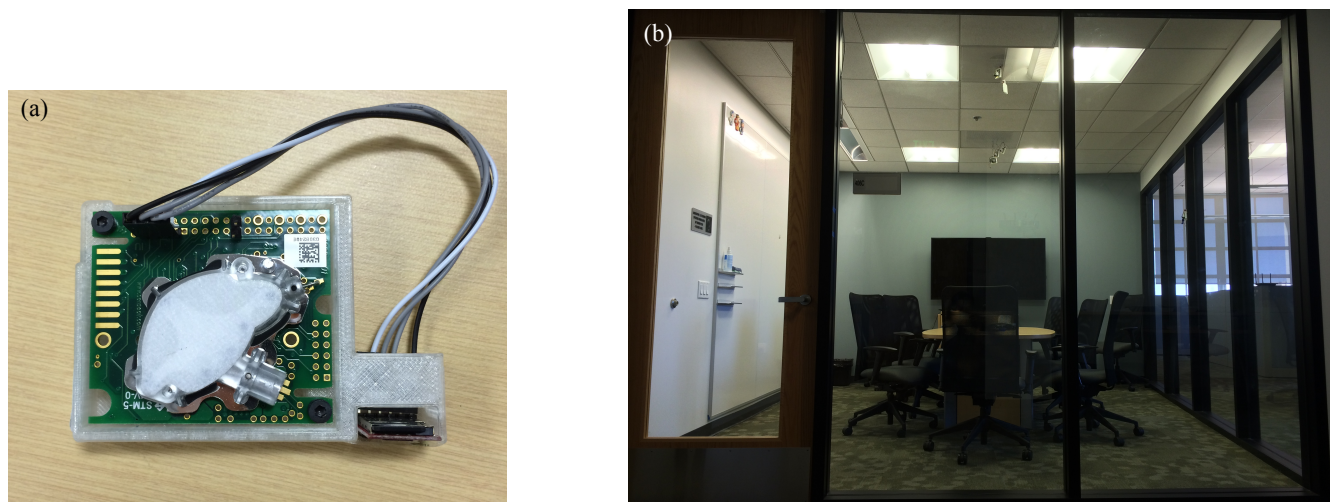


Figure 2. (a) CO<sub>2</sub> sensor up close. The platform is integrated with the main module to sense CO<sub>2</sub> concentration, and a local data storage solution with SD card. (b) The testbed is a conference room located at the Center for Research in Energy Systems Transformation (CREST) in Cory Hall on the UC Berkeley campus. The space is of size  $14 \times 10 \times 9$  ft<sup>3</sup>, equipped with a full ventilation system including an air return vent and air supply vent, as illustrated in Figure 1.

### B. Testbed Deployment

We implemented the experiments in a typical conference room, shown in Figure 2, located at the Cory Hall on the UC Berkeley campus, whose occupancy is demand-based and not regular. The room bears close resemblance to other typical indoor spaces, with a ventilation system including air supply and air return vents on the ceiling. The sensors are placed on both vents, in addition to the blackboard on the sidewall.

### C. Experiments

Two types of experiments are performed, namely CO<sub>2</sub> pump and occupants experiments, with different focuses.

For the CO<sub>2</sub> pump experiments, an outlet placed  $\sim 20$ cm above the desk injects beverage-grade CO<sub>2</sub> through a 200W personal heater to emulate warm human breaths. The experiment is designed with two purposes. First, we want to examine the spatial dependence of CO<sub>2</sub> concentration in the room. Second, we can collect data to identify the parameters of the model whose output matches the measured data, under different frequency of excitation. Hence, we conducted experiments with the pump alternating between ON and OFF states, with the length of a full period of 30min (A), 1hour (B), 3hours (C), and 10hours(D), whose results are detailed in Section IV.

For the occupants experiments, the purpose is to validate sensing by proxy in a real setting. Hence we performed both controlled experiments (E) and field measurements (F,G). Our excitation procedure for the controlled experiments consists of adding or removing one of two participants of the experiment, and noting the time that the occupancy changes. The subjects are graduate students with similar physique. The door is closed during the experiment, while the participants are engaged in normal activity such as working on their computers and talking to each other. The field measurements require much less commitment from the occupants, who are using the conference room for meetings or group study. The occupancy schedules for E, F, G are demonstrated in Figures 5 and 8.

## IV. RESULTS AND DISCUSSION

In this section, we report results from experiments and simulation, and the performance of sensing by proxy in occupants experiments.

### A. Experimental Results and Data Analysis

As described in the section of experimental design, we performed two groups of experiments, namely, one with CO<sub>2</sub> pump and the other with varying number of occupants. Based on the measurements, we make qualitative and quantitative analysis as a preparation.

#### 1) CO<sub>2</sub> pump experiments:

**Hypothesis:** when the CO<sub>2</sub> is injected for a long time with constant emission rate, the system reaches steady state.

The steady-state characterization experiment is conducted, when the pump is turned on for 5 consecutive hours. Figure 3 illustrates the measurements from the supply vent, return vent, and blackboard.

The rate of CO<sub>2</sub> concentration starts to decrease after few hours, and reaches a plateau in the last hour. The steady state concentration settles at around 1200 ppm as a result of mixing of fresh incoming air and CO<sub>2</sub> release.

**Hypotheses:** when the CO<sub>2</sub> is released periodically, the measurement exhibits periodic patterns according to the PDE-ODE system. Further, besides transient behavior due to changes of ventilation rate, the CO<sub>2</sub> concentrations from different points in the room react the same, albeit with different magnitudes.

Both the short period and long period excitation experiments are performed, with the periods of 30 minutes (15min ON, 15 min OFF, same for the following), 1 hour, and 3 hours, as shown in Figures 4 and 7.

As can be seen the CO<sub>2</sub> concentrations at all the sensed locations are responsive to the periodic injection, though the measurement at the air supply vent has a smaller magnitude compared with blackboard and the air return vent. While the CO<sub>2</sub> accumulates from the start of the injection, the first

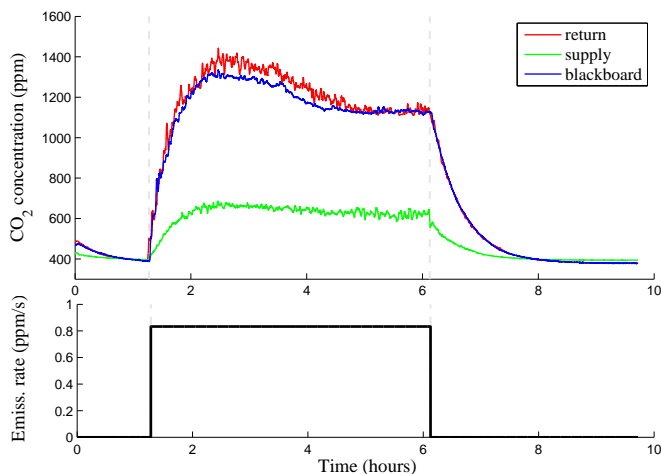


Figure 3. CO<sub>2</sub> pump experiment D. The measured CO<sub>2</sub> concentration from different locations for a 5-hour CO<sub>2</sub> release are shown.

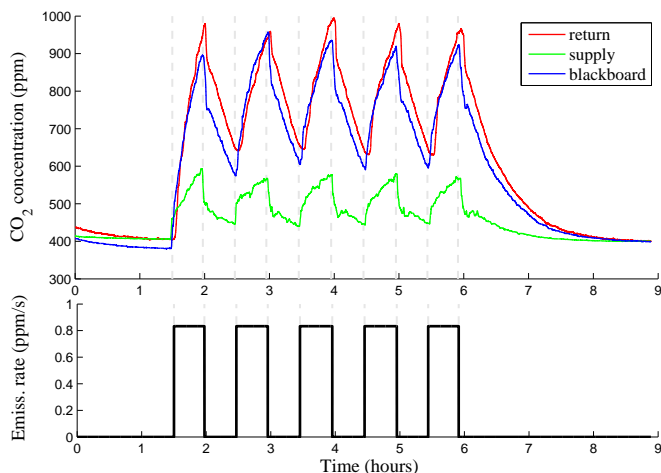


Figure 4. CO<sub>2</sub> pump experiment B. Short term excitation with period of 1 hour. Measurements at return (red), supply (green) vents, and blackboard (blue) are shown.

order derivative decreases as the room reaches higher CO<sub>2</sub> concentration.

To quantitatively evaluate the spatial dependencies of sensors in the room, we now derive the cross-correlation between measurements from three different locations for the CO<sub>2</sub> pump experiments. The definition of the cross-correlation  $r_{y_1 y_2}$  between two signals  $y_1, y_2$ , that is employed here is given by

$$r_{y_1 y_2} = \frac{\sum_{k=1}^T (y_1(k) - \bar{y}_1)(y_2(k) - \bar{y}_2)}{\sqrt{\sum_{k=1}^T (y_1(k) - \bar{y}_1)^2 (y_2(k) - \bar{y}_2)^2}} \quad (17)$$

where  $\bar{y}_1$  and  $\bar{y}_2$  are the sample mean of  $y_1$  and  $y_2$  respectively. The cross-correlation is a measure of the degree of linear dependency between two signals, and hence, it is a meaningful measure for comparing the measurements from different locations inside the room. The values of the cross-correlations are shown in Table I. One can observe that the cross-correlation between return and blackboard measurements is high, whereas

TABLE I. CROSS-CORRELATION VALUE OF CO<sub>2</sub> MEASUREMENTS AT DIFFERENT LOCATIONS FOR EXPERIMENTS A, B, C.

| Location          | Cross-correlation |
|-------------------|-------------------|
| Return-Supply     | 0.9592            |
| Return-Blackboard | 0.9882            |
| Supply-Blackboard | 0.9635            |

the cross-correlations that involve supply measurements are lower. This implies that the signals have a high degree of linear dependency (note that when  $y_1(k) = c_1 y_2(k) + c_2$ , for all  $k$ , the cross-correlation is one) on each other, although the correlation with the supply measurements is lower due to the ventilation operation. Note that the cross-correlation between any two locations is derived as the average cross-correlation obtained from the measurements of the experiments.

## 2) Occupants experiments:

As sensing by proxy aims at accurately infer occupancy through proxy measurements, in addition to CO<sub>2</sub> pump experiments, occupants experiments are necessary to validate our methodology.

As described in the experimental design, we perform strictly controlled and field experiments. The former implements a designed schedule of occupancy, and requires the occupants to sit in designated chairs and remain in the room during the experiment, while allowing them to be engaged in normal activities, such as using computers and chatting. The latter is taken during daily events and requires much less commitment from the occupants.

The following shows results from several such experiments, which substantially cover the usage of the conference room, and can be easily extended to other areas in the building. The field measurements are shown in Figure 5 and 8 (right), and the strictly controlled experiment is illustrated in Figure 8 (left). Note that to avoid significant overlap between graphs of this section and those of the simulation section, we arbitrarily decide which graphs show the blackboard measurement and the others show the simulated return, as long as the evidence is sufficient to for the argument.

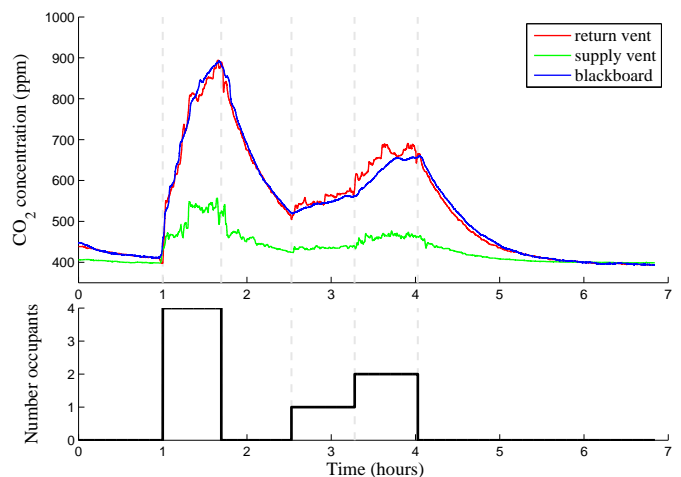


Figure 5. Occupants experiment F. Field measurements during project discussion. Top: Proxy measurements. Bottom: Corresponding occupancy.

Similar to the pump experiment, CO<sub>2</sub> concentration in-

increases almost immediately at the start of occupancy, and the concentration level and rate have a clear correspondence to the number of occupants in the room. The possibility of relating proxy measurements, namely CO<sub>2</sub> concentration, to latent factors, namely occupancy, lays the foundation for sensing by proxy.

Though the system is responsive to the change of occupancy, the time it takes to accumulate or deplete CO<sub>2</sub> to the corresponding stationary value is fairly long. From vacancy to a high level occupancy, the measurement slowly sweeps across several intermediate levels. The difficulty of most distribution-based classification methods is illustrated in Figure 6, where the significant overlapping of regions and misplacement of modes corresponding to different levels of occupancy will lead to confusion for standard machine learning algorithms. By modeling the temporal and spatial dynamics of the system, as we demonstrate in the subsequent sections, we can develop an inference method that is both robust to noise and responsive to change of occupancy.

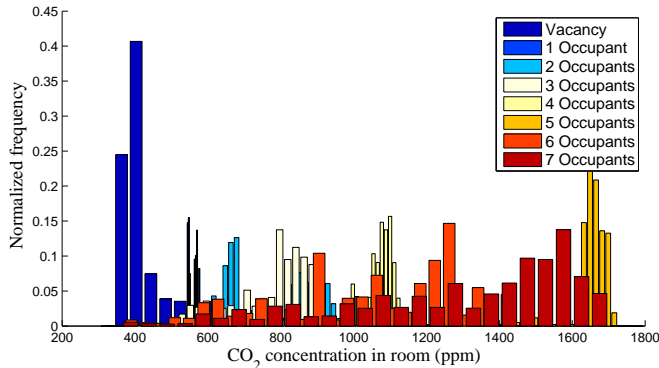


Figure 6. Empirical distribution of CO<sub>2</sub> concentration for all occupants experiments corresponding to different occupancy (color coded).

### B. Simulation with Proxy Link Model

This section applies the model as described by (1)-(4), which links the location-specific proxy measurements to latent CO<sub>2</sub> emission factors to the CO<sub>2</sub> pump experiments and occupants measurements. In particular, we are concerned with the reproduction of the return vent measurements  $u(1, t)$ , i.e., the output of the system, given the supply vent measurements  $U(t)$  and emission rate  $V(t)$ .

The results are illustrated in Figure 7, where two experiments from CO<sub>2</sub> pump measurements are arbitrarily shown since the results are very similar. The set of parameters for the group of CO<sub>2</sub> pump experiments is determined by visual evaluation of the matching of simulation to the air return measurements, which is listed in Table II. The process of parameter evaluation is actually very simple, given the derived equation for stationary distribution

$$u^{\text{stationary}} = U_{\text{stationary}} + \frac{b_X V}{ab} \quad (18)$$

according to the link model (1)-(4), where  $V$  is the fixed emission rate.

The stability of the CO<sub>2</sub> system can be seen in the good matching of all the air return vent measurements. There are,

TABLE II. PHYSICAL PARAMETERS OF PROXY LINK MODEL USED IN ALL THE CO<sub>2</sub> PUMP EXPERIMENTS (A, B, C, D)

| Physical parameter                          | Symbol        | Value |
|---|---------------|-------|
| Convection coefficient ( $\frac{1}{100s}$ ) | $b$           | 2.5   |
| Source coefficient ( $\frac{1}{100s}$ )     | $b_X$         | 1.00  |
| Time constant of human effect (100s)        | $\frac{1}{a}$ | 16.67 |
| Pump emission rate (ppm/sec)                | $\rho_{pump}$ | 0.833 |
| Equilibrium concentration in air (ppm)      | $U_e$         | 400   |

TABLE III. PHYSICAL PARAMETERS OF PROXY LINK MODEL USED IN ALL THE OCCUPANTS EXPERIMENTS (E, F, G)

| Physical parameter                          | Symbol        | Value |
|---|---------------|-------|
| Convection coefficient ( $\frac{1}{100s}$ ) | $b$           | 2.5   |
| Source coefficient ( $\frac{1}{100s}$ )     | $b_X$         | 1.50  |
| Time constant of human effect (100s)        | $\frac{1}{a}$ | 16.67 |
| Human emission rate (ppm/sec)               | $V^H$         | 0.183 |
| Equilibrium concentration in air (ppm)      | $U_e$         | 400   |

nevertheless, occasionally over- and under- matching, especially around the peak and valleys, which might be caused by the fluctuation of ventilation rates. The mismatch, even though not frequent, might introduce bias in our emission rate and occupancy estimations as we show in the next section. It is, therefore, recommended to examine the cause of the mismatch in actual building operations and periodically calibrate the model in order for sensing by proxy to make the most reliable inference. It is also possible to design an automatic calibrator for each distributed sensor system.

Based on our experiences in the CO<sub>2</sub> pump experiments, we designed occupants controlled and field experiments to collect occupancy ground truth and validate our link model in practice, as shown in Figure 8.

In actual building usage, especially conference rooms and common areas, the occupancy is often irregular, as exemplified by the experimental profiles. The simulation of proxy measurements, therefore, is direct estimation of the effects of the irregular change of latent factors. The closeness of simulation matching to actual proxy measurements, as can be seen, is a clear indication of the accuracy of the link model, and also ensures reliable inference of latent factors. The spatial and temporal simulation is illustrated in Figure 9.

As a general remark, our proxy link model is extremely simple and parsimonious with parameters. The set of parameters, including the convection coefficient  $b$ , the source coefficient  $b_X$ , time constant of human effects  $\frac{1}{a}$ , in addition to the human emission rate  $V$  and CO<sub>2</sub> concentration of fresh air  $U_e$ , which are standard fixed parameters, are shared among all the experiments in the same group of CO<sub>2</sub> pump and occupants experiments, with relatively small difference between different groups due to the extent of emulation by the pump to human breathing. This makes our model extremely easy to train and employ in practice. The additional advantage of parsimonious model relies on its stability and robustness by avoiding the potential overfitting problem. As we demonstrate next, the sensing by proxy approach substantially outperforms other popular methods and yet remains physically meaningful.

### C. Proxy Inference of Occupancy

The observer model as described by (5)-(8) and Algorithm 1 are applied in this section to infer the CO<sub>2</sub> emission rate and occupancy based on proxy at return and supply vents.

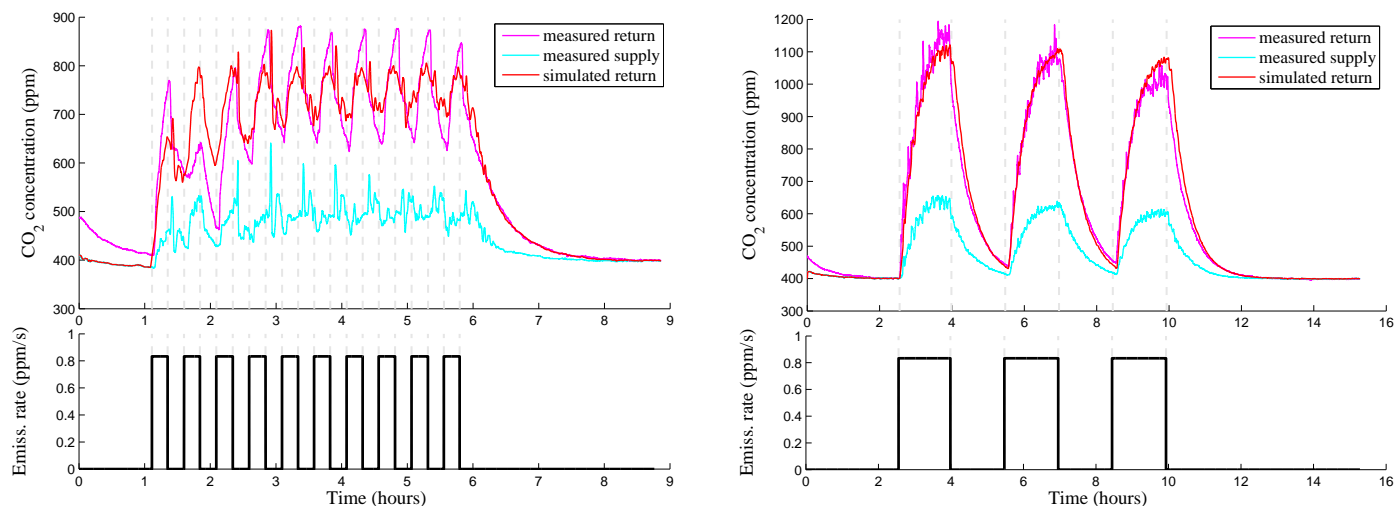


Figure 7. Proxy model simulation with CO<sub>2</sub> pump experiment A with 30 minutes (left) and experiment B with 1 hour (right) periodic excitation. Measurements at supply (green), return (blue), and simulated return (red) vents are shown.

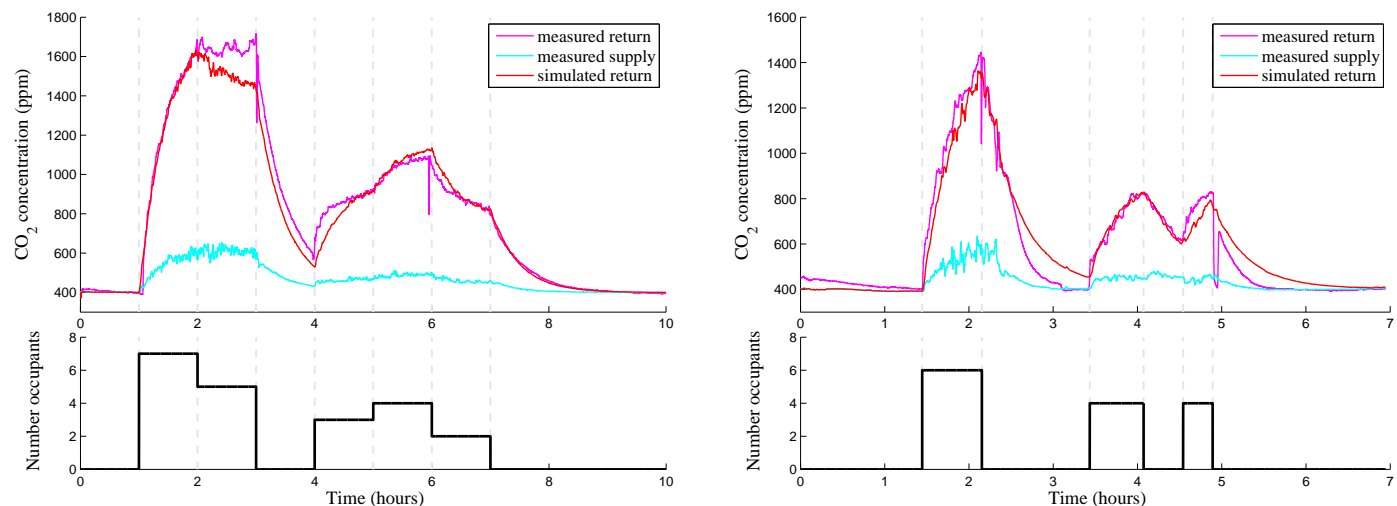


Figure 8. Proxy link model simulation with occupants experiment E (left) and G (right). The proxy measurements at return (blue), supply (green), and simulated return (red) vents are demonstrated.

Sensing by proxy distinguishes from other machine learning methods that assumes independence of samples by implicitly considering time-autocorrelation of the latent emission rate. The advantage as a result is to have smooth state trajectory after simple signal processing, where we employed median filter directly on the estimated emission rate,  $\hat{V}$ , with a window of 8min for Experiment A, 20min for B and C, and 25min for all the occupant experiments. The median filter is a useful denoising method in signal processing, which is often preferred to mean filter to preserve relevant details and sharp transitions in the trace, as we will demonstrate next. Figure 10 is plotted for the CO<sub>2</sub> pump experiment with periods of 30 minutes and 3 hours, respectively.

Contrary to the common belief that CO<sub>2</sub>-based methods are slow in response, sensing by proxy exhibits fast response to the change of occupancy. The previous argument is based on the fact that it takes time to accumulate CO<sub>2</sub> to a level

that can be detected, and this accumulation time is fairly long as we observed in the experiments. During the accumulation, the concentration value sweeps across the stationary values for lower occupancy when several people enter the room, or those for higher occupancy when people leave, which account for the significant overlap in the histograms of CO<sub>2</sub> concentration in Figure 6.

Sensing by proxy, however, tackles this issue by modeling the dynamics of the measurements based on our link model, which implicitly considers the increasing rate and stationary values to infer the actual occupancy. As a result, sensing by proxy is immediately responsive to changes of occupancy even when the transition is fairly frequent in the case of Figure 10 (left), which is not possible with other methods since the concentration remains at a relatively high level even when the pump is turned off. The parameters chosen for the estimation are  $L_1 = 2$ ,  $L_2 = 0.02$ , and the other physical parameters of

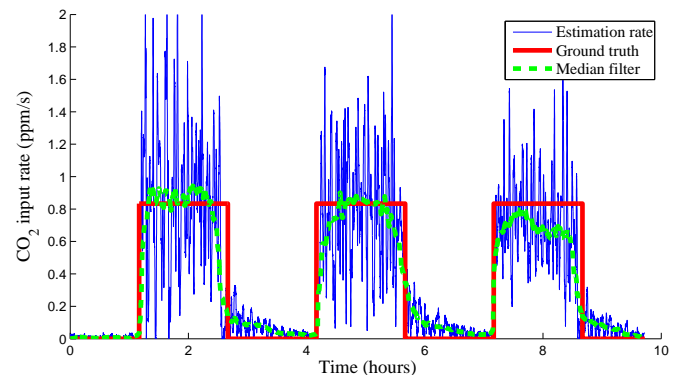
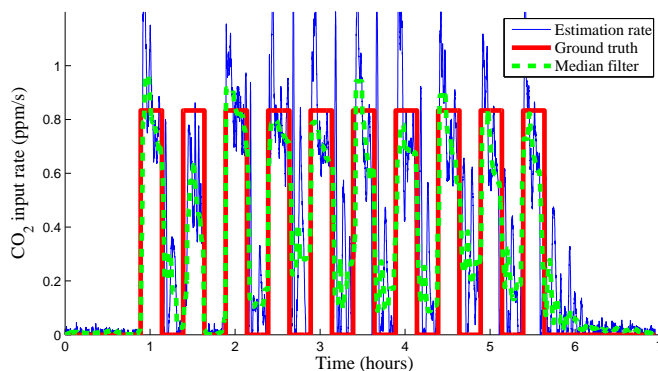


Figure 10. Sensing the latent CO<sub>2</sub> emission rate by proxy for CO<sub>2</sub> pump experiment A (left) and experiment C (right). The estimated emission rate (blue), median filtered rate (green), and ground truth (red) are given.

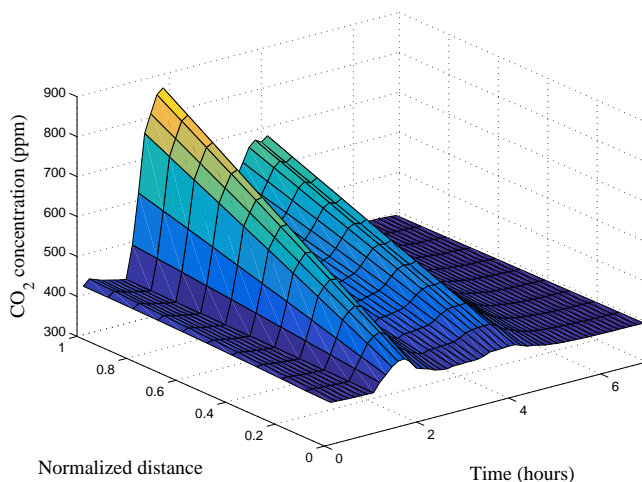


Figure 9. Spatial and temporal dynamics of CO<sub>2</sub> concentration as represented as the states in the proxy link model.

the model are shown in Table II.

In the case of occupants estimation, the task is more difficult due to the following reasons. First, humans are not uniform in physique, so the emission rate must vary for different occupants. Second, the positions of the people sitting in the room are arbitrary, which might question our assumption that the human emission has uniform effect on measurements on the ceiling regardless of positions of sources. Also, the ventilation rate, opening and closing of doors, and different activities might all introduce additional noise to the measurements. Nevertheless, regardless of these factors, Figure 11 shows that sensing by proxy is reasonably robust to these influences, where we plot the estimated number of occupants together with the ground truth.

The fast transition behavior exhibited in the CO<sub>2</sub> pump experiments is also observed for the occupants experiments, even without any sensors to explicitly sense the exits or entry of people as in other methods such as particle filters or Markov models [8]. The occupancy inference is accurate without explicitly specifying the transition rates of the occupancy model. For all these inference, the parameters chosen are the same, namely  $L_1 = 2$ ,  $L_2 = 0.02$ , and physical parameters from

Table III.

To compare with other models, we employ the root mean-squared-error (RMSE) with units of fractional people, given by

$$RMSE = \sqrt{\frac{1}{T} \sum_{k=1}^T (\phi(k) - \hat{\phi}(k))^2} \quad (19)$$

where  $\phi(k)$  is the ground truth occupancy at time  $k$ ,  $\hat{\phi}(k)$  is the estimated occupancy at time  $k$  given by

$$\hat{\phi}(k) = \left\lfloor \frac{\tilde{V}(k)}{\rho_{\text{human}}} + \frac{1}{2} \right\rfloor \quad (20)$$

where  $\tilde{V}(k)$  is the median-filtered estimated emission rate at time  $k$ ,  $\rho_{\text{human}} = 0.183\text{ppm/sec}$  is the average sedentary person emission rate, and  $\lfloor x \rfloor$  is the floor operation to obtain the largest integer smaller than  $x$ .

The comparison of sensing by proxy with other methods are shown in Table IV. Since all the other models require substantial training phase, the data is split to training and testing sets and the RMSE is computed by 10-fold cross-validation. The algorithms take the measurements from the air supply and air return vents as features, where the corresponding labels are the number of occupants. The outputs for each testing point are the number of occupants obtained by classification, which are compared against the ground truth. For standardization purpose, we employ the Weka Machine Learning Toolkit [14] for the implementation of these algorithms. No time dynamic models, such as particle filters are learned for comparison, as it requires additional sensors to measure transitions and extra knowledge of transitional probabilities, which require substantial learning data and might not be reliable for the case of non-stationary activities in practice.

Even though the parameters of our link model are shared across all the experiments, the training for other models might be significantly different for each experiments, which differ by scale and time. Therefore we decide to separate the RMSE for each experiment, as shown in the first three columns of Table IV, which might make it obvious that which model is consistently better even with different dataset. In the last column, we combine all the occupants experiments data and test each model. Note that as it is possible for other models

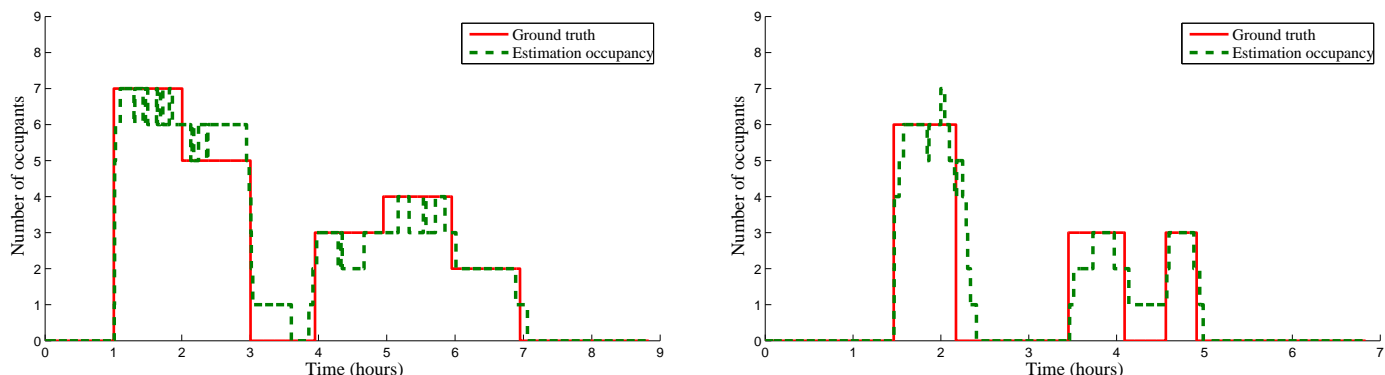


Figure 11. Occupancy detection by “sensing by proxy” (Algorithm 1) for experiment E (left) and G (right). The response times from vacancy to occupancy and vice versa are about 10 seconds and 5 to 10 minutes respectively, since the method detects the dynamics of the system rather than static concentration. The estimations (green) are within 1 occupant of the ground truth (red).

TABLE IV. COMPARISON OF ROOT MEAN-SQUARED ERROR OF ESTIMATION IN OCCUPANTS EXPERIMENTS

|                        | Exp. E        | Exp. F        | Exp. G        | Mixed         |
|------------------------|---------------|---------------|---------------|---------------|
| Naïve Bayes            | 1.3080        | 0.7454        | 1.7457        | 1.3555        |
| Bayes Net              | 1.2345        | 0.6555        | 1.5406        | 1.2061        |
| Logistic regression    | 1.0796        | 0.6109        | 1.8414        | 1.4736        |
| Multi-Layer Perceptron | <u>0.9686</u> | <u>0.5672</u> | 1.6221        | 1.2321        |
| RBF Network            | 1.0837        | 0.6760        | 1.6496        | 1.3341        |
| Seq. Min. Opt. (SMO)   | 1.2326        | 0.6185        | 1.8803        | 1.6118        |
| AdaBoostMI             | 1.6415        | 0.7053        | 2.2257        | 2.3927        |
| Sensing by Proxy       | <b>0.5922</b> | <b>0.3809</b> | <b>0.7331</b> | <b>0.6311</b> |

to yield different outputs due to different training, sensing by proxy will output the same value given the chosen parameters, which is desirable since it is less susceptible to training noise.

Sensing by proxy, as can be seen, delivers standout performance in all the testings, while the second best (underlined) positions are shared between Multi-Layer Perception (MLP) and Bayes Net, whole error metric almost doubles that of sensing by proxy in the mixed dataset case. By ignoring the dynamics of CO<sub>2</sub> concentration, these algorithms are confused by the overlapping concentration region as shown in Figure 6 especially during CO<sub>2</sub> accumulation and depletion period.

Close examination of the confusion matrix for our model and the second best model, in the mixed dataset case, the Bayes Net, as visualized in Figure 12, reveals an additional advantage of sensing by proxy. In the illustration, the size of the bubble represents the percentage of data classified as  $\hat{\phi}$  (y-axis) for ground truth  $\phi$  (x-axis), normalized for the sample size corresponding to  $\phi$ . Bayes Net has a straight diagonal pattern, but it is undermined by the nonnegligible points far off the diagonal, representing misclassification error with large magnitude. On the contrary, sensing by proxy, though not possessing the straight diagonal pattern as in Bayes Net, is fairly clean of points far off the diagonal region. The point mass is also concentrated in the narrow band of sub-diagonals, which indicate that the estimation is within an error of 1 person. This is clearly preferred in practice, as sufficiently accurate estimation of occupancy can save much more energy than exact occupancy estimation but with misinference of crowded space when the room is just vacant.

## V. RELATED WORK

Existing approach to indoor occupancy estimation employed machine learning methods with multi-sensor fusion through dense sensor deployment. Passive Infrared (PIR) sensors and magnetic reed switch to detect door open/close events are suitable for binary occupancy detection [3]. Fusion of PIR sensors with cameras in the particle filter framework was proposed for occupancy prediction. Inhomogeneous Markov Chain, such as closest distance Markov chain and Blended Markov Chain, was employed for real-time occupancy based conditioning strategies [7]. Occupancy estimation using real (motion, door closure) and virtual (PC activity detector) sensors was presented in a small office based on the decision tree and artificial neural network models [15]. Individual presence detection based on power consumption using zero-training algorithm is proposed in [16]. A complex sensor network was established [8] comprising ambient-sensing (lighting, temperature, relative humidity, motion detection and acoustics), CO<sub>2</sub> sensing, and air quality sensing systems, which were incorporated into a Hidden Markov Model.

There are two main streams of modeling room air dynamics, namely computational fluidic dynamics (CFD) and zonal models [17]. CFD requires substantial model specification (e.g., locations of all walls, furniture, and occupants) and computation to produce detailed map of air motion. Zonal models, on the contrary, relies on ODE mass balance laws between different zones, though the distributed local nature of airborne contaminant transfer within a single space is not captured. Clearly a trade-off between spatial details and model simplicity is more practical for occupancy sensing.

Techniques for the estimation of the concentration of contaminants emitted from a source in indoor environments exist in the literature [17]. Boundary observers for some classes of PDEs are constructed in [18] via backstepping. In [19], this methodology is applied for the estimation of the state-of-charge of batteries. Observer designs for time-delay systems with unknown inputs are presented in [20]. In light of the current development in control theory, sensing by proxy recasts the occupancy inference as a problem of state and input estimation to allow robust, automatic, real-time inference.

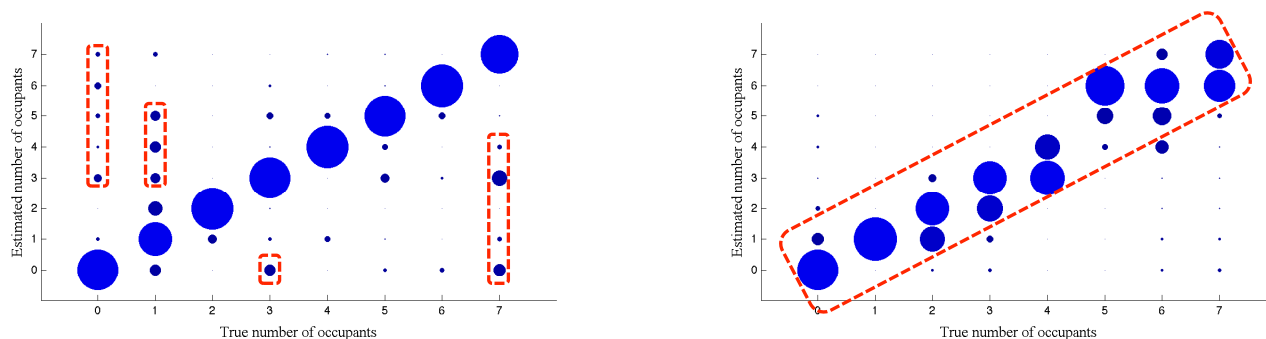


Figure 12. Visualization of confusion matrix for Bayes Net (left) and sensing by proxy (right), where the position of circles represents the true number of occupants (x-axis) and estimated number of occupants (y-axis), and the size indicates the percentage normalized for each column.

## VI. CONCLUSION

This study describes an occupancy detection algorithm using indoor CO<sub>2</sub> concentration based on the sensing by proxy methodology, which explores the spatial and temporal features of the system with constitutive models. Controlled field experiments are conducted in a typical indoor space to show that the proposed link model can reproduce the CO<sub>2</sub> measurements given the latent emission rates. It is demonstrated that sensing by proxy can reliably detect the number of occupants based on “proxy” observations with RMSE of 0.6311 (fractional person), as compared to 1.2061 (fractional person) of the best alternative machine learning algorithm. Investigation of the confusion matrices reveals that the estimation by sensing by proxy is within 1 occupant of the ground truth with high probability, while the estimation by Bayes Net sometimes has large deviations. By successfully identifying the L3 factors (location, latent factors, and link model) in the problem, sensing by proxy can be also applied to other tasks, such as indoor pollutants source identification, while requiring minimal capital investments.

## ACKNOWLEDGMENT

This research is funded by the Republic of Singapore’s National Research Foundation through a grant to the Berkeley Education Alliance for Research in Singapore (BEARS) for the Singapore-Berkeley Building Efficiency and Sustainability in the Tropics (SinBerBEST) Program. BEARS has been established by the University of California, Berkeley as a center for intellectual excellence in research and education in Singapore.

## REFERENCES

- [1] J. McQuade, “A system approach to high performance buildings,” United Technologies Corporation, Tech. Rep., 2009.
- [2] V. Garg and N. Bansal, “Smart occupancy sensors to reduce energy consumption,” *Energy and Buildings*, vol. 32, no. 1, 2000, pp. 81–87.
- [3] Y. Agarwal, B. Balaji, R. Gupta, J. Lyles, M. Wei, and T. Weng, “Occupancy-driven energy management for smart building automation,” in *Proceedings of the 2nd ACM Workshop on Embedded Sensing Systems for Energy-Efficiency in Building*. ACM, 2010, pp. 1–6.
- [4] J. Lu et al., “The smart thermostat: using occupancy sensors to save energy in homes,” in *Proceedings of the 8th ACM Conference on Embedded Networked Sensor Systems*. ACM, 2010, pp. 211–224.
- [5] V. L. Erickson et al., “Energy efficient building environment control strategies using real-time occupancy measurements,” in *Proceedings of the First ACM Workshop on Embedded Sensing Systems for Energy-Efficiency in Buildings*. ACM, 2009, pp. 19–24.
- [6] S. Meyn, A. Surana, Y. Lin, S. M. Oggianu, S. Narayanan, and T. A. Frewen, “A sensor-utility-network method for estimation of occupancy in buildings,” in *Decision and Control, 2009 held jointly with the 2009 28th Chinese Control Conference. CDC/CCC 2009. Proceedings of the 48th IEEE Conference on*. IEEE, 2009, pp. 1494–1500.
- [7] V. L. Erickson, S. Achleitner, and A. E. Cerpa, “Poem: Power-efficient occupancy-based energy management system,” in *Proceedings of the 12th international conference on Information processing in sensor networks*. ACM, 2013, pp. 203–216.
- [8] B. Dong et al., “An information technology enabled sustainability test-bed (itest) for occupancy detection through an environmental sensing network,” *Energy and Buildings*, vol. 42, no. 7, 2010, pp. 1038–1046.
- [9] S. Wang and X. Jin, “Co2-based occupancy detection for on-line outdoor air flow control,” *Indoor and Built Environment*, vol. 7, no. 3, 1998, pp. 165–181.
- [10] A. Baughman, A. Gadgil, and W. Nazaroff, “Mixing of a point source pollutant by natural convection flow within a room,” *Indoor air*, vol. 4, no. 2, 1994, pp. 114–122.
- [11] N. Bekiaris-Liberis and M. Krstic, “Lyapunov stability of linear predictor feedback for distributed input delays,” *Automatic Control, IEEE Transactions on*, vol. 56, no. 3, 2011, pp. 655–660.
- [12] M. Krstic and A. Smyshlyaev, *Boundary control of PDEs: A course on backstepping designs*. Siam, 2008, vol. 16.
- [13] “K-30 10,000 ppm CO2 sensor,” <http://www.co2meter.com/products/k-30-co2-sensor-module>, June 2015.
- [14] M. Hall, E. Frank, G. Holmes, B. Pfahringer, P. Reutemann, and I. H. Witten, “The weka data mining software: an update,” *ACM SIGKDD explorations newsletter*, vol. 11, no. 1, 2009, pp. 10–18.
- [15] S. Srirangarajan and D. Pesch, “occupancy estimation using real and virtual sensors,” in *Proceedings of the 12th international conference on Information processing in sensor networks*. ACM, 2013, pp. 347–348.
- [16] M. Jin, R. Jia, Z. Kang, I. C. Konstantakopoulos, and C. Spanos, “Presencesense: Zero-training algorithm for individual presence detection based on power monitoring,” in *BuildSys14*, November 5–6, 2014, Memphis, TN, USA, 2014, pp. 1–10.
- [17] L. Mora, A. Gadgil, and E. Wurtz, “Comparing zonal and cfd model predictions of isothermal indoor airflows to experimental data,” *Indoor air*, vol. 13, no. 2, 2003, pp. 77–85.
- [18] A. Smyshlyaev and M. Krstic, “Backstepping observers for a class of parabolic pdes,” *Systems & Control Letters*, vol. 54, no. 7, 2005, pp. 613–625.
- [19] S. Moura, N. Chaturvedi, and M. Krstic, “Pde estimation techniques for advanced battery management systems part i: Soc estimation,” in *American Control Conference (ACC)*, 2012. IEEE, 2012, pp. 559–565.
- [20] D. Koenig, N. Bedjaoui, and X. Litrico, “Unknown input observers design for time-delay systems application to an open-channel,” in *Decision and Control, 2005 and 2005 European Control Conference. CDC-ECC’05. 44th IEEE Conference on*. IEEE, 2005, pp. 5794–5799.